



Assessment of the Greenland ice sheet - atmosphere feedbacks for the next century with a regional atmospheric model fully coupled to an ice sheet model

Sebastien Le clec'h¹, Xavier Fettweis², Aurelien Quiquet¹, Christophe Dumas¹, Masa Kageyama¹, Sylvie Charbit¹, Coraline Wyard², and Catherine Ritz³

¹Laboratoire des Sciences du Climat et de l'Environnement, LSCE/IPSL, CEA-CNRS-UVSQ, Université Paris-Saclay, F-91191 Gif-sur-Yvette, France

²Laboratory of Climatology, Department of Geography, University of Liège, Liège, Belgium

³Univ. Grenoble Alpes, CNRS, IGE, F-38000 Grenoble, France

Correspondence to: Sebastien Le clec'h (sebastien.leclech@lsce.ipsl.fr)

Abstract. In the context of global warming, the projected Greenland sea level rise contribution is mainly controlled by the interactions between the Greenland ice sheet (GrIS) and the atmosphere, in particular through the temperature and surface mass balance – elevation feedback. In order to evaluate the importance of these feedbacks, we used three methods to represent the interactions between the GrIS model GRISLI and the polar regional atmosphere model MAR, under the RCP 8.5 scenario from 2020 to 2150. In the simplest method, there is no coupling, MAR computes varying atmospheric conditions using a constant GrIS geometry (topography and extent) set to observations and GRISLI is forced by these results. The second is a one-way coupling method which represents the interactions by correcting offline the MAR outputs to account for topography changes computed by GRISLI. The third method is a full two-way coupling in which the ice sheet topography and extent seen by the atmospheric model evolve after each ice sheet model time step. Due to the ice sheet elevation feedback, the two-way coupling method amplifies the projected decrease in surface mass balance, the increase in surface temperature and the GrIS surface thinning for the coastal regions, compared to the no coupling method. Compared to both the one-way and the no coupling methods, the two-way coupling allows the changes of fine scale processes to be represented, such as the increase in katabatic winds over the coast. As a consequence, in 2150, the two-way coupling method computes a GrIS melting contribution to sea level rise 9.3 % larger than the no coupling method, and 2.5 % larger than the one-way coupling methods. After 150 years, the GrIS extent seen by MAR in the two-way method is 52 400 km² lower than with the no coupling method. Furthermore, in 2150, using a fix ice sheet mask, as in the no coupling method, overestimates by 24 % the SLR contribution from SMB compared to the use of the ice sheet mask as simulated in the two-way method. Beyond the century time-scale, a two-way method becomes necessary in order to avoid an underestimation of the projected ice sheet volume, topography and ice extent reduction. The one-way coupling method however seems to be sufficient to represent the interactions for projections until the end of the 21st century. The no coupling method always underestimates the projected ice sheet volume loss significantly due to the lack of feedback between the GrIS and the atmosphere.



1 Introduction

The Arctic is the region of the Earth experiencing the largest increase in temperature since the pre-industrial era (Serreze and Barry, 2011), with consequences already perceptible on the mass evolution of the polar ice caps and the Greenland ice sheet (Rignot et al., 2011). The atmospheric conditions control the variability of the near-surface temperature (ST) and the surface mass balance (SMB) of the GrIS. The SMB represents the difference between snow accumulation, which is further transformed into ice, and the ablation, which are processes of ice loss. Accumulation and ablation are both sensitive to ST. Variations of ST and SMB directly affect the GrIS total ice mass by impacting its characteristics such as thickness, ice volume and ice extent. In turn, variations of the GrIS characteristics affect the ST and the zones of ablation ($SMB < 0$) and accumulation ($SMB > 0$). GrIS changes can also disrupt the atmospheric circulation over Greenland caused by changes in topography thermal contrast between ice sheet surface and atmosphere layers, surface albedo and ice sheet area, as shown by Vizcaino et al. (2015), Vizcaíno et al. (2008) and Lunt et al. (2004). Quantifying the balance between these different processes and feedbacks is required to understand and predict more confidently the evolution of the GrIS under current and future global warming.

Although numerous studies highlighted the importance of correctly representing the interactions between the GrIS topography changes and the atmosphere (Vizcaino et al., 2015; Edwards et al., 2014a; Alley and Joughin, 2012; Huybrechts et al., 2002), only few global or regional models have taken the GrIS topography changes into account to compute the future evolution of the SMB, ST and energy budget over the GrIS. The climate models usually represent the ice sheet component with a fixed and constant topography, even under a warm transient climate forcing. Recently, Vizcaino et al. (2015) used an atmosphere-ocean general circulation model (AOGCM) coupled with an ice sheet model (ISM) to explore topography feedbacks on ice mass loss. They found an ice mass loss amplification of 8–11 % (by 2100) and of 24–31 % (by 2300). Since both their ice sheet and climate models have a relatively coarse resolution (3.75° for the atmospheric component and 10 km for the ice sheet model), they focus on the added value of incorporating the coupled processes and less on exactly reproducing the observed GrIS, which would require more detailed physics in both models. They explain that their study must be regarded as a necessary first step towards more advanced coupling of ice sheet and climate models at higher resolution. Indeed, a higher resolution is necessary to represent correctly the steep slopes at the ice sheet margins (typically, the altitude varies by 2000 m over distances of the order 100 km). However, the computation of atmospheric fields at a resolution similar to the ISM one requires large computing resources. Franco et al. (2012) developed an interpolation method allowing to correct each SMB component (snowfall, rainfall, run-off, sublimation and evaporation) as a function of topography changes. They showed that their corrective method is able to significantly reduce the model output differences between a coarse spatial resolution model and a high resolution model. Edwards et al. (2014a) developed an alternative parametrisation of the interactions between the GrIS and the atmosphere to correct the SMB computed by a regional atmospheric model (RCM) by taking into account the GrIS topography changes computed by an ISM. This method only requires limited additional supercomputing resources. Under the SRES A1B emissions scenario, Edwards et al. (2014b) showed that a larger melting of the GrIS is obtained when the elevation feedback is taken into account (ranging from 4.4 % in 2100 to 9.6 % in 2200). However, in both parametrisations by Franco et al. (2012) and Edwards et al. (2014b), the authors only consider a strict linear relationship between topography



and SMB changes.

5 These previous studies show that one of the first requirements to improve the representation of the feedbacks between the GrIS and the atmosphere is to use a high resolution atmospheric model and a detailed snow model. The higher resolution allows to better represent the elevation gradients and therefore the steep topography and the extent of the ablation zone. Together with the higher resolution, the detailed snow model can also better estimate the GrIS surface properties, such as albedo, snow cover and surface melting. Furthermore an RCM developed for the Greenland region can represent more complex atmospheric and land surface processes prevailing specifically over this area such as blowing snow (Gallée et al., 2001) or bare ice albedo (Box et al., 2012).

10 The second fundamental requirement is to represent the ice sheet topography changes in the atmospheric model by using an ISM instead of the fixed geometry usually used. This can be done by using a full coupling between the RCM and the ISM. More than twenty ice sheet models exist, and are currently compared in the Ice Sheet Model Intercomparison Project (Nowicki et al., 2016). They represent thermodynamical and physical processes of the Greenland ice sheet with different levels of complexities (Gagliardini et al., 2013; Saito et al., 2016). They all compute the dynamical response of the GrIS to a given climate forcing which can be, for example, the SMB and the ST fields computed by RCMs (or global models). However, as SMB and ST from the climate models do not take into account the GrIS evolution, the climate forcing used by the ISM could be flawed.

15 In order to explicitly represent the feedbacks between the GrIS and the atmosphere at high resolution and to evaluate their impacts on the SMB, ST and topography changes as well as on the SLR GrIS contribution, we coupled the "polar" regional climate model MAR (for Modèle Atmosphérique Régional, in French, Fettweis et al. (2017)) and the high resolution ISM GRISLI (for GRenoble Ice Shelf and Land Ice Ritz et al. (2001) Philippon et al. (2006)) and Alvarez-Solas et al. (2011a). To further investigate the representation of the interactions between the GrIS and the atmosphere, we compared experiments using the tow-way coupling method (called hereafter 2-W for two-way coupling) with two other experiments using less complex methods. In the first method (referred to as NC for no coupling), the atmosphere-GrIS feedbacks are not represented; in the second method (referred as 1-W for one-way coupling), the feedbacks are partially represented using the Franco et al. (2012) corrective method but without any physical coupling between MAR and GRISLI.

20 A description of the atmospheric model, the ice sheet model and the climate forcing is given in Sect. 2. Sect. 3 focuses on the description of the three methods (2-W, 1-W and NC) considered in this study, on the initialisation and the experimental set-up. In Sect. 4, we describe the results of the NC experiment. Next we compare the 2-W experiment with the NC and 1-W experiments, in terms of atmospheric and ice dynamic fields and of the GrIS ice extent. Sect. 5 focuses on the limit of using the NC or the 1-W method instead of the 2-W method. These sections are followed by the discussion and the main conclusions of this study.



2 Models and experiments

2.1 The MAR atmospheric model

MAR is a regional atmospheric model fully coupled with the land surface model SISVAT which includes a detailed snow energy balance model (Gallée and Duynkerke, 1997). It has been developed to simulate the GrIS SMB and has been extensively validated against in situ observations (Fettweis et al., 2017). The horizontal resolution is 25 km x 25 km covering the Greenland region (6600 grid points) from 60°W to 20°W and from 58°N to 81°N. The model has 24 levels for the atmospheric layer from the surface to 16 km high. SISVAT has 30 levels to represent the snowpack (with a depth of at least 20m over the permanent ice area) and 7 levels for the soil in the tundra area. Lateral boundary conditions can be provided either by reanalysis dataset (such as ERA-interim or NCEP) to reconstruct the recent GrIS climate (1900-2015) (Fettweis et al., 2017) or by general circulation models (GCMs) to perform future projections such as those used for the last IPCC report (e.g. Fettweis et al. (2013)). MAR uses the solar radiation scheme of Morcrette et al. (2008). The representation of the hydrological cycle (including a cloud microphysical model) is based on Lin et al. (1983) and Kessler (1969). The snow-ice part comes from the snowpack model *Crocus* (Brun et al., 1992). This 1-D model simulates fluxes of mass and energy between snow layers, and reproduces snow grain properties and their effect on surface albedo. The present work uses MAR version 3.6. The differences with previous MAR versions used in Fettweis et al. (2013, 2017) are only related to adjustments of some parameters in cloudiness and bare ice albedo. The bare ice albedo has been improved by parametrising the melt ponds impact on the albedo.

2.1.1 Boundary conditions and climatic forcing

The topography of the GrIS as well as the surface types (ocean, tundra and permanent ice) are provided by Bamber et al. (2013). At its lateral boundaries, MAR is forced every 6 hours with atmospheric fields (temperature, humidity, wind and surface pressure) and surface oceanic conditions (sea surface temperature and sea ice extent) coming from reanalyses or from GCM outputs. As a result, the atmospheric circulation simulated by MAR over the Greenland ice sheet is strongly dependent on the quality of the climatic fields computed by GCMs or reanalyses as an input to the model. Fettweis et al. (2013) have shown that forcing GCMs which satisfactorily simulate the present-day free-atmosphere mean summer temperature at 700 hPa and the large-scale circulation over Greenland at 500hPa are best suited to force MAR. For the present study we therefore choose to force MAR with the MIROC5 model output (Watanabe et al., 2010), because it has been shown by Fettweis et al. (2013), to be the best choice to reproduce the present-day climate with respect to the results of MAR forced by reanalyses, compared to the other GCMs from the CMIP5 data-base. The greenhouse gas forcing used in MAR (scenario RCP8.5) is the same as that used in the MIROC5 simulation (Watanabe et al., 2010).

30



2.1.2 Model initialisation and experiment

Before starting our experiments, MAR needs to be properly initialised to limit spurious drifts, which would introduce unwanted trends in the results. The snowpack included in *SISVAT* requires more than 6 years to reach an equilibrium with atmospheric fields. Here, we initialise MAR by running it with the atmospheric forcing fields from MIROC5 from 1970 until 1976 and by
5 using the present-day GrIS geometry provided by Bamber et al. (2013). This first simulation uses a *SISVAT* initial state from a previous similar MAR-MIROC5 simulation. In this paper, the MAR results will be analysed for the period following year 1976.

After the initialisation period, and for all experiments, MAR is forced by transient MIROC5 atmospheric fields of the CMIP5 historical (1970-2005) and RCP8.5 scenarios (Taylor et al., 2012) until 2100. In order to extend the MAR experiment until
10 2150, we have repeated the MIROC5 year 2095 (representative of the years 2090s) for 50 additional years.

2.2 The GRISLI Ice sheet model

The GRISLI (GRenoble Ice Shelf and Land Ice) is a coupled ISM first developed to compute the dynamical evolution of the Antarctic ice sheet (Ritz et al., 2001; Philippon et al., 2006; Alvarez-Solas et al., 2011a). It has then been successfully applied
15 to the northern hemisphere ice sheet (Peyaud et al., 2007; Alvarez-Solas et al., 2011b; Quiquet et al., 2013; Charbit et al., 2013). In the present work, we used a 5 km resolution grid covering the Greenland ice sheet with 301x561 grid points. GRISLI is a three-dimensional hybrid thermo-mechanically coupled ISM computing the temporal evolution of the ice sheet, which is a function of the surface mass balance, ice flow and basal melting (Eq. 1):

$$\frac{\partial H}{\partial t} = -\nabla(\bar{U}H) + M - b_{melt} \quad (1)$$

20 where t is time, H the ice thickness, \bar{U} the depth-averaged horizontal velocity, M the surface mass balance and b_{melt} is the basal melting.

The ice flow is governed by using both the shallow ice (Hutter, 1983) and shallow shelf (MacAyeal, 1989) approximations to solve the Stokes equations (Ritz et al., 2001). The SIA (shallow ice approximation) assumes that ice flow is caused only by
25 vertical shear stress, neglecting the longitudinal stresses. This assumption is only valid for slow flowing ice. For fast flowing regions vertical shearing becomes smaller than longitudinal shearing and the SSA assumption, which neglects the vertical stresses, is used. The SIA component of the computed ice sheet velocity is mainly controlled by the ice sheet surface slope while the SSA component is mainly controlled by the ice flux and basal dragging. Using both approximations in one model allows to better represent the different rheologies found in an ice sheet. In GRISLI, the SSA velocity is used as a sliding velocity
30 (Bueler and Brown, 2009) when the basal temperature is at the ice melting point. In this case, the basal drag follows a standard power law relating the basal velocity to the basal shear stress with a basal drag coefficient. For cold base conditions, the sliding velocity is set to zero. The resulting velocity for every model grid point is the addition of the SIA and SSA components. For



floating ice points (ice shelves), we assume no basal drag. In addition, if the ice thickness of the floating ice shelves is under 250 m and if no neighbouring points are grounded, the point is removed and the corresponding ice mass loss is considered as a calving flux. Determination of the grounding line position is based on a floating criterion.

The sliding velocity is constrained by the topography and the characteristics of the Greenland bedrock. GRISLI also represents the deformation rate via the Glen flow law corrected by an enhancement factor to mimic the effect of ice anisotropy. The isostatic adjustment in response to ice load is governed by the flow of the asthenosphere with a characteristic time constant of 3000 years and by the rigidity of the lithosphere. The model is thermo-mechanically coupled and the temperature field is computed both in the ice and in the bedrock by solving a time-dependent heat equation.

2.2.1 Boundary conditions and climatic forcing

To compute the vertical properties of the GrIS, such as velocity and temperature, GRISLI only needs surface and bottom boundary conditions and surface climatic forcing. The annual mean near surface air temperature together with the geothermal flux (Maule et al., 2009) is used to compute the ice vertical temperature profile. To represent the GrIS initial topography and ice extent, we use boundary conditions from Bamber et al. (2013) and the Greenland Ice Mapping Project (Howat et al., 2014). The climatic forcings are from the MAR-MIROC5 experiment. At the bottom of the ice sheet we use the bedrock topography from Bamber et al. (2013). for this study, the basal drag coefficient is also a boundary condition. It is computed during the GRISLI initialisation step. This initialisation follows an optimized spin-up method (Le clec'h et al., in prep) based on data assimilation of the surface velocity field from Joughin et al. (2010) (see Sect. 2.2.2).

2.2.2 Model initialisation and experiment

Due to the approximation and parametrisation used to solve the physical equations, it is necessary to equilibrate GRISLI with the initial boundary conditions (surface, bottom and vertical, before performing sensitivity experiments. Le clec'h et al. (in prep) optimised a data assimilation method applied to GRISLI by using the present-day observed surface velocities, topography and climate forcing to obtain a GRISLI initial state. This method, similar to that used in Gillet-Chaulet et al. (2012), allows to avoid an initial adjustment of the model to the boundary conditions during the initial years of the simulation, which could be misinterpreted as due to climate forcing.

In the Greenland ice sheet, the characteristics of the ice just over the bedrock are poorly known and they are likely to change with space and time. Basal characteristics, such as basal sliding, have a crucial impact on ice sheet motion (Boulton and Hindmarsh, 1987; Weertman, 1957). As a result any error in the basal velocity computation can spread vertically in the ice and generate slowdown or acceleration of ice sheet motion. In GRISLI, the basal velocity is mostly influenced by the choice of the basal drag coefficient. We used an inverse method to infer the basal drag coefficient from observed surface velocities. Our computation of the basal drag coefficient is done in three main steps:

- The first step is a relaxation run of 200 years using initial conditions which are not necessary consistent between them (first guess of the basal drag from Edwards et al. (2014a), surface and bottom ice sheet characteristics from Bamber et al.



(2013), vertical fields from Gillet-Chaulet et al. (2012)). For this step, GRISLI is forced by the 1976-2005 mean climate from MAR-MIROC5. Then, in order to have an ice flux as close as possible to observation, we calculate offline an ice surface velocity corrected by a factor representing the difference between the observed ice thickness of Bamber et al. (2013) and the GRISLI computed ice thickness (after 200 model years). If topography differences tend to be positive (resp. negative), the factor allows to decrease (resp. increase) the surface ice velocity in order to reduce the gap between observed and computed ice flux.

– In the second step, we perform another GRISLI simulation using the same initial conditions, the same forcing fields and set of parameters as in the first step. However, during the first 20 years, instead of using the fixed initial basal drag coefficient, we use an iterative process to calculate each year a new basal drag value. To do that, we compare the corrected velocity fields calculated in the first step (hereafter the target velocity) to the one simulated for a specific basal drag. Depending on the ratio of the computed velocity and the target velocity, we compute a new coefficient that allows to increase or decrease the sliding for the following year. After the first 20 years, we stop calculating the coefficient and let the GRISLI simulation to evolve freely over 200 years more with the last computed basal drag.

With the initial conditions used for this study we need to repeat 8 times this second step in order to obtain a constant minimum gap between the computed and the observed GrIS thickness.

– The third step allows to make the ice vertical profile of temperature consistent with the climate forcing used. Here the mean climate forcing is the same as the one used in previous steps. This 3rd step is necessary due to the long time scale that temperature takes to be in equilibrium with the others fields. For this long experiment we perform a 30 000 years simulation where topography is kept constant during the entire experiment. All the other vertical fields (such as velocity and temperature) evolve through time. At the end of this long experiment we obtain a new set of initial conditions in which the ice sheet is in equilibrium with the climate forcing. However, because the velocity fields change (due to the evolving temperature) we compute a last basal drag coefficient over 20 years following a process similar to the second step.

We use the resulting final conditions (thickness, temperature, velocity and basal drag) as conditions for all the following experiments of this study.

In order to validate the final GrIS conditions obtained after the last spinup experiment, we perform a new GRISLI run using these conditions and the same mean 1976 - 2005 climate forcing coming from MAR. To obtain a final GrIS thickness as close as possible to observations, we use the Bamber et al. (2013) thickness as surface initial condition. After evolving freely over 2000 years, the GrIS volume drift each year by 0.0014 % (0.01 mm in equivalent SLR). We then consider that the computed GrIS characteristics and dynamics reach an equilibrium with the mean climate forcing used. Despite of this equilibrium, the thickness difference between the GrIS computed at the end of the GRISLI initialization (after 2000 years of relaxation) and the GrIS observed by Bamber et al. (2013) reaches a median anomaly value equal to +28 m and ranges on average over all the ice sheet, between -83 m (5th quantile) and +211 m (95th quantile). This result has been compared with other model results within



the framework of an intercomparison project of initialisation methods (initMIP project). It turned out that GRISLI is one of the models that compares the best with observations (Goelzer et al., 2017).

3 Coupling methods and experiments

In this study, we compare three methods of different complexities to account for the atmosphere – GrIS interactions. We investigate how these methods affect the computed SMB, ST, SLR contribution and surface elevation changes. For the three methods described below, MAR is forced every 6 hours at its lateral boundaries by the MIROC5 fields and run at a 25 km resolution from 1976 to 2100. The forcing fields from MIROC5 evolve in response to the historical (until 2005) and the RCP8.5 scenarios (from 2006 to 2100).

Before forcing GRISLI with the 25 km resolution SMB and ST outputs from the MAR model, we need to spatially interpolate them onto the 5 km GRISLI grid. However, as SMB and ST are very sensitive to the Greenland topography we also need to correct them by the topography changes due to the difference of resolution between MAR (25 km) and GRISLI (5 km). Using a linear interpolation method if the steep topography at the GrIS margin and the complex orographic features in these areas are not taken into account could lead to important biases in SMB and ST in these regions (Franco et al., 2012).

In the present study, for all the experiments, we first interpolate the MAR outputs on the 5 km GRISLI grid using a simple bilinear interpolation. Then, the fields are corrected for the altitude difference induced by the difference of resolution between MAR and GRISLI. These topography corrections are based on the method developed by Franco et al. (2012) who derive a local vertical gradient of SMB (or ST) as a function of altitude for each GRISLI grid point. This gradient is then used to compute the correction due to the difference of altitude between the Bamber et al. (2013) topographies seen by MAR (resolution 25 km) and by GRISLI (resolution 5 km). This procedure can be followed at a daily time scale (Noël et al., 2016). For our purpose, we choose to average the daily vertical gradients at the annual time scale and to apply the altitude correction every year.

For all the experiments described below, the coupling between MAR and GRISLI starts in 2020 when the SMB anomalies are large enough to induce significant topography changes in GRISLI.

We investigate three levels of coupling between the ice sheet and the atmospheric models:

- The "No Coupling" method (hereafter referred to as NC). The present-day GrIS geometry (topography and ice extent) provided by Bamber et al. (2013) is prescribed to MAR as a boundary condition during the entire simulation duration. GRISLI is forced until 2150 (see Sect. 2.1.2) using the downscaled MAR outputs described above. The NC method does not allow to account for the ice sheet feedback on the climate. Rather, it provides the response of GrIS under a specific climate forcing.
- The "One-way coupling" method (hereafter called 1-W). This method goes a step further. It is based on the same principle as the NC method, but the SMB and ST fields are corrected based on an updated altitude ($H(t)$) given by (Eq. 2):

$$H(t) = H_{Bamber} + \Delta H_{GRISLI}(t) \quad (2)$$



where H_{Bamber} is the Bamber et al. (2013) topography at 5 km and ΔH_{GRISLI} is the topography anomaly simulated by GRISLI between the initial topography computed for year 2000 from the equilibrium state ($t=0$) and the ongoing time step (t). In doing so, this method artificially accounts for the elevation feedback because the SMB and ST are initially computed by MAR on a fixed ice sheet topography. With this method GRISLI is forced off-line by the MAR atmospheric conditions already computed in the NC run, therefore allowing sensitivity experiments in GRISLI with limited additional computer time. However, the changes in GRISLI topography are not taken into account by MAR.

- The Fully Coupled method (hereafter 2-W). This coupling method is the most accurate way to represent the interactions between the GrIS and the atmosphere but it is also more computationally expensive. At the end of a MAR simulated year, MAR is paused and GRISLI is forced by the 5 km interpolated SMB and ST just computed by MAR. GRISLI then computes a new GrIS topography and extent which are aggregated on to the 25 km MAR grid for the simulation of the next year of the MAR experiment. GRISLI and MAR are never stopped, just alternatively paused and resumed until 2150.

The differences between the GRISLI equilibrium state after the initialisation step and the observed topography (Bamber et al., 2013) (cf Sect. 2.2.2) could lead to inconsistencies between the results obtained by MAR under its usual setup, i.e. calibrated with the Bamber et al. (2013) topography, and the results that would be obtained by using directly the GRISLI topography. For this reason, in both the 2-W and the 1-W experiments, we use anomalies of GrIS topography applied on Bamber et al. (2013) topography rather than the absolute topography from GRISLI.

4 Results

4.1 The uncoupled simulation: the NC experiment

4.1.1 MAR

The mean ST over the first two decades (2000-2020) and averaged over the whole GrIS is equal to -18.7°C and the mean SMB to 434 Gt yr^{-1} (Fig. 1). After 2020, the ST increases by $0.065^{\circ}\text{C yr}^{-1}$ until 2100 (Fig. 1). Over the same period (2020-2100), the averaged GrIS SMB decrease by 12.3 Gt yr^{-1} (Fig. 1). The surface temperature anomaly in 2100 compared to 2000 shows a warming ranging from $+1.5^{\circ}\text{C}$ in the southern part of the GrIS to more than $+8^{\circ}\text{C}$ in the northern part (Fig. 2A). This warming in northern Greenland is a direct response to the MIROC5 forcing fields due to the polar temperature amplification. However, regional heterogeneities are observed in the annual mean GrIS SMB spatial distribution (Fig. 2B). Indeed, between 2000 and 2100 there is a positive SMB anomaly (i.e. more ice accumulation) in a zone located along a South-North transect in the central part of the GrIS. This ice accumulation is mainly governed by the larger snowfall on the GrIS central part in winter and spring seasons (not shown). An opposite, trend 10 times larger than ice accumulation, is simulated over the edges of the ice sheet, with a negative SMB (i.e. ice ablation). In these regions, the summer season governs this negative SMB and is characterised by larger rainfall and melting ice (meltwater and runoff increase) than for other seasons (not shown). As a



consequence, the limit between the accumulation ($SMB > 0$) and ablation ($SMB < 0$) areas, also called the equilibrium line altitude (ELA, a line where $SMB = 0$), shifts inland through time (Fig. 3). This shift explains the mean decrease of SMB over the whole GrIS until 2100 seen in Fig. 1.

4.1.2 GRISLI

5 In 2100, a decrease of 15.8 m in mean ice sheet thickness is simulated (Fig. 2C) with a standard deviation of 32.7 m. In 2150, the mean ice thickness decrease reaches 38.6 ± 68.4 m. We can distinguish two types of regions: there is a thinning over the GrIS coastal regions and a thickening over the central GrIS regions (Fig. 2C). The thickness changes for the 2000-2150 period show the same patterns as the 2000-2100 period, but with a larger magnitude. Over the thinning regions, between 2000-2100 (resp. 2000-2150) the ice thickness decreases by 40 ± 32.5 m (resp. 78.5 ± 70 m). On the contrary, in central regions, the ice
10 thickness increases with a median value of 4.4 ± 12 m (resp. 7.8 ± 13.4 m). The thickness anomaly is due to the complex combination of changes both in surface atmospheric conditions and ice dynamics conditions.

The ice dynamics is impacted by the warming climate. Generally, the simulated ice velocities increase from the central part of the ice sheet to the coastal regions (Fig. 4A). However, at the ice sheet margins, the ice velocities strongly decrease. In GRISLI, the fine scale structure of the Jakobshavn (western coast) and the Kangerlussuaq (eastern coast) glaciers is relatively
15 well reproduced (Fig. 5A-B). For these glaciers and their associated ice-streams, within 100 years, the surface velocities slow down by more than 200 m yr^{-1} in the coastal regions, while they increase by more than 60 m yr^{-1} in the interior (Fig. 5C-D). Because the region feeding the ice stream has a frozen base, the SIA assumption is the predominant simplification used by GRISLI to compute the ice velocities. In this area, the ice velocity increase is due to the SIA velocity component (Fig. 5E-F). As mentioned previously, by 2100, the thickness decreases at the margins and increases in the interior (Fig. 5K-L), resulting in
20 steeper slopes and thus in larger SIA velocities. However, the coastal regions have a temperate base and the SSA component of the velocity is predominant. Thus, the ice flow velocity is mainly controlled by the ice flux coming from the inland part. As the ice flux depends on the ice thickness which decreases over the coastal areas, the SSA velocity component decreases (Fig. 5G-H). This increase-decrease ice velocity pattern has been also reported by Peano et al. (2017), using GRISLI forced by CMIP5 models under the RCP8.5 scenario.

25 As a result of ice accumulation-ablation changes and ice velocity changes, the ice mask (numbers of grid points covered by permanent ice) decreases by 3.7 % in 2100 compared to the initial one (in 2000-2005). During the first 20 years (2000-2020), the total GrIS volume remains stable with no additional contribution to SLR compared to year 2000. After 2020, the GrIS volume decreases, resulting in a global contribution of +7.6 cm in 2100.

Extending the GRISLI NC experiment until 2150, forced by the same 2095 MAR forcing climate results in an amplification of
30 all the changes observed in 2100 and discussed above: the extent of the ablation zone, the larger thinning and the slow down ice velocities in the coastal regions. As a consequence, the GrIS contribution to global SLR is amplified, reaching +18.7 cm in 2150.



4.2 Differences between the 2-W and the NC experiments.

4.2.1 Impact on SMB and ST

The near-surface temperature (ST) simulated for 2150 in the 2-W experiment over the whole GrIS is warmer than in the NC experiment, except in the region at the edge of the GrIS, which is strongly colder (until -10°C , Fig. 6A). The ST of this region is sensitive to the atmospheric circulation. At the edges of the ice sheet, there is an intensification of the strong and cold katabatic winds coming from the central part of the GrIS in 2-W compared to NC. The katabatic winds have a daily time scale resolution and are represented by the MAR model (Gallée and Pettré, 1998; Gallée et al., 1996). These stronger winds are due to the higher coastal surface slope simulated in 2-W than in NC (see Sect. 4.2.2). As a consequence, they prevent warmer and wetter air from the ice-free areas (i.e. covered by tundra) and ocean from reaching the GrIS margin regions (van den Broeke and Gallée, 1996). Thus, the ST decrease over the edges of the GrIS (Fig. 6A). The second consequence of the strengthening of the katabatic winds is to enhance the atmospheric exchange at the middle of the slope over the GrIS. Indeed, at the surface, the lower atmospheric pressure generated by the stronger katabatic winds is filled in by the warmer air coming from higher atmospheric levels in the boundary layer. Thus the warming of the upper part of the boundary layer combined with the lower surface elevation, explains the ST increase on the coastal regions inland from the very edge of the ice sheet. These two types of colder and warmer regions simulated in 2-W with respect to NC are already present after 100 years of experiment (Fig. S1A-B).

In 2150, the SMB difference between the 2-W and NC experiments exhibits two distinct patterns. With the 2-W approach, the SMB increases by 0.6 m yr^{-1} over the eastern coast, the south central part and in some local regions in the northern part of the GrIS (Fig. 6B). These regions are characterized by a larger snowfall in winter season compared to the NC experiment. The processes explaining these increased SMB regions are probably linked to the strengthening of the atmospheric circulation along the Greenland eastern coast coming from northern latitudes, thus bring wetter and colder mass air. Despite these regions of positive SMB anomalies in 2150, the pattern in the SMB difference between 2-W and NC is generally a negative anomaly ranging from -2.3 m yr^{-1} to -0.4 cm yr^{-1} over the coastal areas of the GrIS. Following the decrease of the ST, the surface snow melting cumulated with less snowfall and more precipitation falling as rain instead of snow drive this SMB patterns. As a result, in 2150, there is a decrease of 112 Gt yr^{-1} of ice over the ablation area in 2-W with respect to NC, and, over the accumulation area, the simulated SMB in the 2-W experiment is 23 Gt yr^{-1} lower than the one simulated in the NC experiment. In 2100, the SMB anomaly shows the same patterns as the 2150 SMB pattern, but with lower magnitude (Fig. S1A). Over the ablation zone, the mean value of the SMB anomalies increases by a factor of 10 between 2050 and 2150 (see Table 1).

The SMB changes have an impact on the extent of the ablation zone. This area increases with time and, at the end of the simulation is 14 % larger in 2-W than in NC (Table 1). As a result, the ELA shifts more inland, in 2-W, by +12 km in the north eastern GrIS (wrt NC, Fig. 3).



4.2.2 Impact on thickness and ice dynamics

The patterns of the surface elevation changes between the 2-W and the NC experiments (Fig. 6C) follow the SMB anomaly patterns. Over the eastern coast, southern central part and locally in some regions on the northern part of Greenland, the ice thickness increases, reaching more than 10 m in some locations such as East Greenland (Fig. 6C). This increasing ice thickness is explained by a larger positive SMB and a lower surface temperature over these regions. The second anomaly pattern is found all along the Greenland coast, where a decrease of the ice thickness is found in areas of lower ST and in the ablation zone. The main changes occur on the western edge of the GrIS where the thinning between 2-W and NC reaches more than -25 m (Fig. 6C). Further inland, there is a smaller thinning (-0.2 ± 3 cm in average after 150 years). As a result, averaged only over the entire ablation area, the thinning after 150 model years is equal to 9.0 ± 11.1 m (see also Table 2). These ice thickness anomaly patterns are observable, with lower magnitude, when comparing 2-W and NC after 100 years (Fig. S1C).

The main consequence of the increased thinning in coastal regions is the increase of the surface slope between the central part and the margin of the ice sheet. Increased surface slopes results in stronger katabatic winds. Furthermore, the thinnest parts of the GrIS become ice or snow-free or snow free, exhibiting bare ice and modifying albedo feedbacks, with a decrease of the surface albedo which amplifies the GrIS melting.

The ice dynamics computed by GRISLI are also impacted by the full representation of the interactions. Compared to the NC experiment, the ice velocities simulated with the 2-W experiment show a succession of positive and negative anomalies (Fig. 4B). The ice velocities increase from the central part of the GrIS to the coastal regions. The increase-decrease velocity pattern is amplified in the 2-W compared to the NC because of the larger thickness anomaly and follows the same processes than explain in Sect. 4.1.2.

20

4.2.3 Impact on SLR contribution and ice sheet area

After 150 model years, the melting contribution to global SLR reaches +20.4 cm in the 2-W experiment. In comparison, the melting obtained in the NC experiment is equivalent to a SLR of +18.5 cm. This difference (Fig. 7) is linked to the better representation of the interactions between the GrIS and the atmosphere. The coupling allows for a better representation of the processes occurring at the margin, and in particular the ice sheet margin retreat. As a result of ice melting, GrIS coastal grid points can become ice free. The GrIS extent in the 2-W experiment is reduced by 52 400 km² compared to the NC experiment and increases exponentially with time (Table 1). Thus, the ice sheet mask field, which represents the ice coverage percentage of each grid cell of the grid used by the models, and which is therefore dependent of the ice sheet extent, decreases with time (Fig S2B).

To evaluate the projected GrIS melting contribution to SLR, the SMB integrated over the ice-covered areas (i.e. the sheet mask field) is often used (Fettweis et al., 2013). However, this method could lead to strong uncertainties in the SLR contribution obtain. For example, using the NC result in 2150, if we integrate the SMB over the no updated ice sheet mask (as in the NC method), we calculate an integrated SMB 158 Gt yr⁻¹ lower than using the updated ice sheet mask simulated by GRISLI (as



in the 2-W method). This higher integrated SMB, obtained when using no updated ice sheet mask, is only explain by taking into account the GrIS regions becoming ice free compared to the updated ice sheet mask. We show that using a fixed ice sheet mask (as in NC) leads to a large overestimation of the contribution to SLR calculated from SMB.

5 4.3 Differences between 2-W and 1-W experiments.

Anomalies of ST, SMB and surface elevation for the averaged 2145-2150 period between the 2W and the 1W experiments present similar features (Fig. 8) than those obtained between the 2W and the NC experiments, but with lower magnitude. Over the coastal regions, a larger increase in ST is obtained with 2-W as well as a lower SMB and a larger decrease in surface elevation (Fig. 8), hence highlighting the role of the feedbacks between the ice sheet and the atmosphere that are taken into account in 2-W but not in NC. As an example, the katabatic wind feedback preventing the prepenetration of warm air results in colder 2-W ST compared to 1-W.

In 2150, the GrIS SLR contribution obtained in the 1-W experiment reaches +19.9 cm, i.e 0.5 cm less than in the 2-W experiment (Fig. 7). Although this difference seems quite low, the local altitudes changes are larger in 2-W than in the 1-W experiment. Indeed, even if the median value of the ice thickness anomalies (2-W vs 1-W) between 2000 and 2150 are quite similar (respectively 73.3 m and 72.4 m), some regions show stronger surface anomalies (Fig. 8A). Scatter plots of surface elevation anomalies between 2-W and NC (red dots), 1-W and NC (green dots) and 2-W and 1-W (blue dots) as a function of the ice sheet altitude show the spatial variability of the ice thickness response to warming climate (Fig. 9A). The 2-W method yields negative and positive anomalies relative to NC, while the 1-W method mainly yield s negative values (relative to NC). For both experiments, the regions where the ice thickness is under 1000 m are the most impacted by the warming climate. For these lower to medium altitude points, there is a strong variability of surface elevation anomalies. Thus, for the 2-W experiment, the anomalies range between +16.4 m (98 % quantile value) and -43.1 m (2 % quantile value). For the 1-W experiment, the surface anomalies range between -1.5 m (98 % quantile value) and -45.2 m (2 % quantile value). Above 1000 m, the higher the altitude, the smaller the surface anomalies (Fig. 9A). The regions at low elevations are the most sensitive to the coupling method and to the warmer climate. This sensitivity to altitude increases with time, and is stronger for the 2-W experiment than for the 1-W experiment (Fig. 9B). High altitude regions are less sensitive to climate changes and to the coupling method used (Fig. 9B).

These thickness changes are correlated with changes in ice ablation and ice accumulation area. After 150 years, the ELA shifts more inland in 2-W than in 1-W (Fig. 3), and the ice ablation area is 11 % greater in 2-W than 1-W after 150 years.



5 Discussion

5.1 Limits of the models

The 5 km grid resolution of GRISLI does not allow represents the smallest peripheral GrIS glaciers to be finely represented. This could limit our results: as we have shown that the coastal GrIS regions are the most sensitive to climate forcing, the GrIS contribution to SLR could be enhanced by increasing the spatial resolution of the ISM in these regions. Furthermore, as we hypothetise an identical basal drag over time, we underestimate the acceleration of the ice flow of the glaciers due to the basal lubrication coming from meltwater or rainfall percolation at depth and reaching the bedrock (Kulesa et al., 2017). An other limit of the GRISLI model is its simple representation of the grounding line position and thus of the buttressing effect which could impact the ice dynamics (Gagliardini et al., 2010). Except for these aspects, GRISLI is a good tool to be coupled in future ESMS in order to take the GrIS evolution into account with a combination of a good representation of the ice dynamics and a limited impact on the added computational resources. As for the ISM, increasing the grid resolution of MAR, would allow to better represents atmospheric-topography feedbacks and more complex atmospheric processes which can have an impact on the SMB in the steep coastal regions. However, as for ice dynamic modeling, the higher is the resolution, the higher is the computational resources needed to produce results.

The absence of any representation of the GrIS-ocean feedbacks is also a limiting factor. Indeed, as the GrIS is an island, several glaciers are in direct contact with the ocean and feedbacks could take place between peripheral glaciers and the ocean. The warm ocean water could accelerate the melting of the glaciers and the added fresh water in the ocean could in turn, have an impact on sea surface temperatures, oceanic circulation and sea-ice cover. The GrIS and the atmosphere evolution could be both modified by this added fresh water flux in the ocean system.

20

5.2 Limits of the methods

The 1-W coupling method neglects the spatial variability of the thickness anomaly and underestimates regional feedbacks compared to the 2-W method. These differences are explained by the linear relationship used, in the 1-W coupling method, to correct the atmospheric fields (SMB and ST) as a function of the surface elevation anomaly, as developed by Franco et al. (2012). Indeed, the relationship between the atmosphere and the GrIS changes is nonlinear because surface elevation changes interact not only with both SMB and ST, but also with all the other atmospheric fields which influence the SMB or the ST directly or indirectly, as for example the winds, the humidity, and the albedo. The 2-W method appears to be the best way to simulated atmospheric-GrIS feedbacks.

If the main objective is to compute the SLR contribution from the entire GrIS without investigating atmospheric or GrIS changes at the regional scale, the use of the 2-W coupling method with a high resolution seems avoidable until 2100. However, over longer time scales, or to study more regional processes changes, the use of a the 2-W coupling method is necessary to represent the local feedbacks between the atmosphere and the GrIS fields and ensure that the SLR contribution is not underestimated by simulating. As an example, the changes in the GrIS extent and ice surface slope have a direct impact on



surface albedo and strength of katabatic winds.

Although the difference in the GrIS melting contributions to SLR between 1-W and 2-W seems low, the use of the 2-W method to compute the ice sheet evolution for 50 additional years (from 2100 to 2150) with the constant forcing of the year 2095 contributes to increase the ice mass loss contribution to SLR by +0.5 cm compared to use of the 1-W method. This volume contribution ranges between 25 % to 100 % of the loss of peripheral Greenland glaciers volume in 100 years derived from the RCP8.5 scenario (Radić et al., 2014; Machguth et al., 2013).

6 Conclusions

In this study, we have improved the representation of the interactions between the GrIS and the atmosphere by developing a full coupling between the Greenland ice sheet model GRISLI and the atmospheric model MAR (2-W experiment). To assess the importance of this improvement, we have investigated the atmosphere and ice sheet responses to the RCP 8.5 warming climate scenario, and we have compared the 150 years of our fully coupled experiment (2-W) with two other experiments using a less complex coupling method (1-W) and a no coupling at all (NC). The fully coupled approach under the RCP 8.5 scenario produces a GrIS melting contribution to SLR of +20.4 cm in 2150, while the 1-W and NC methods produce a GrIS contribution to SLR respectively of +19.9 cm and +18.4 cm, respectively. The difference of 0.5 cm between the 2-W and the 1-W methods represents at least 25 % of the contribution of the peripheral Greenland glaciers melting estimated for the next 100 years using the same RCP 8.5 scenario (Radić et al., 2014; Machguth et al., 2013). This difference, increasing with time, is mainly explained by representation of local interactions between the GrIs and the atmosphere, only possible with the 2-W method. Furthermore, even if the difference is not perceptible in 2100 and it is low in 2150, we have shown that the ice loss computed from the integration of the SMB over a fixed ice sheet mask is 21 % higher than that obtained with the use of an evolving ice sheet mask. This means that most of RCM-based studies have probably overestimated the ice loss computed from a change in SMB.

However, with the 5 km grid resolution of GRISLI, we cannot reproduce the fine-scale structure of the Greenland coast and glaciers. Using an ice sheet model with higher resolution and more complex physics (i.e. Full-Stokes models) and a fully coupled method would probably amplify the sensitivity of these coastal regions. This argument is also valid for the atmospheric model for which a higher resolution would be beneficial for the representation of fine scale atmospheric processes over the ice sheet. We showed that it is at small spatial scales that the coupling method makes most difference. It would therefore be very interesting to find the optimal resolution of the ice sheet and the atmospheric model, for ISM-RCM coupling. Furthermore, since the Greenland ice sheet and glaciers are in contact with the oceanic component, changes in oceanic characteristics, due to the input of freshwater from GrIS melting or due to the warming climate scenario, could in turn disrupt the GrIS and atmosphere evolution. The next step of this study will be therefore to improve the representation of the oceanic component by developing a fully coupled method between an ISM, an RCM and an oceanic model to evaluate the impacts on the Greenland polar region but also on remote regions.



7 Data availability

The model outputs from the simulations described in this paper are freely available from the authors upon request. The source code of MAR version 3.7 is available on the MAR website: <http://mar.cnrs.fr>.

Author contributions. The implementation of the couplings methods was done by X. Fettweiss with the help of C. Wyard. They also performed the simulations. S. Le clec'h analysed the results with the help of A. Quiquet, C. Dumas, X. Fettweis, S. Charbit and M. Kageyama. S. Le clec'h wrote the manuscript in collaboration with S. Charbit, A. Quiquet, M. Kageyama, X. Fettweis, C. Dumas. C. Ritz have developed the GRISLI model and helped with its implementation and initialisation.

Competing interests. The authors declare that they have no conflict of interest.

Acknowledgements. S. Le clec'h, M. Kageyama, S. Charbit and C. Dumas acknowledge the financial support from the French-Swedish GIWA project and the ANR AC-AHC2, as well as the CEA for the PhD funding. A Quiquet is funded by the European Research Council grant ACCLIMATE no 339108. Computational resources (MAR and GRISLI) have been provided by the Consortium des Équipements de Calcul Intensif (CÉCI), funded by the Fonds de la Recherche Scientifique de Belgique (F.R.S.–FNRS) under grant no. 2.5020.11 and the Tier-1 supercomputer (Zenobe) of the Fédération Wallonie Bruxelles infrastructure funded by the Walloon Region under the grant agreement no. 1117545.



References

- Alley, R. B. and Joughin, I.: Modeling Ice-Sheet Flow, *Science*, 336, 551–552, doi:10.1126/science.1220530, 2012.
- Alvarez-Solas, J., Charbit, S., Ramstein, G., Paillard, D., Dumas, C., Ritz, C., and Roche, D. M.: Millennial-scale oscillations in the Southern Ocean in response to atmospheric CO₂ increase, *Global and Planetary Change*, 76, 128–136, doi:10.1016/j.gloplacha.2010.12.004, 2011a.
- 5 Alvarez-Solas, J., Montoya, M., Ritz, C., Ramstein, G., Charbit, S., Dumas, C., Nisancioglu, K., Dokken, T., and Ganopolski, A.: Heinrich event 1: an example of dynamical ice-sheet reaction to oceanic changes, *Climate of the Past*, 7, 1297–1306, doi:10.5194/cp-7-1297-2011, 2011b.
- Bamber, J. L., Griggs, J. A., Hurkmans, R. T. W. L., Dowdeswell, J. A., Gogineni, S. P., Howat, I., Mouginot, J., Paden, J., Palmer, S., Rignot, E., and Steinhage, D.: A new bed elevation dataset for Greenland, *The Cryosphere*, 7, 499–510, doi:10.5194/tc-7-499-2013, 2013.
- 10 Boulton, G. S. and Hindmarsh, R. C. A.: Sediment deformation beneath glaciers: rheology and geological consequences, *Journal of Geophysical Research: Solid Earth*, 92, 9059–9082, 1987.
- Box, J. E., Fettweis, X., Stroeve, J. C., Tedesco, M., Hall, D. K., and Steffen, K.: Greenland ice sheet albedo feedback: thermodynamics and atmospheric drivers, *The Cryosphere*, 6, 821–839, doi:10.5194/tc-6-821-2012, 2012.
- Brun, E., David, P., Sudul, M., and Brunot, G.: A numerical model to simulate snow-cover stratigraphy for operational avalanche forecasting, *Journal of Glaciology*, 38, 13–22, 1992.
- 15 Bueler, E. and Brown, J.: Shallow shelf approximation as a “sliding law” in a thermomechanically coupled ice sheet model, *Journal of Geophysical Research*, 114, doi:10.1029/2008JF001179, 2009.
- Charbit, S., Dumas, C., Kageyama, M., Roche, D. M., and Ritz, C.: Influence of ablation-related processes in the build-up of simulated Northern Hemisphere ice sheets during the last glacial cycle, *The Cryosphere*, 7, 681–698, doi:10.5194/tc-7-681-2013, 2013.
- 20 Edwards, T. L., Fettweis, X., Gagliardini, O., Gillet-Chaulet, F., Goelzer, H., Gregory, J. M., Hoffman, M., Huybrechts, P., Payne, A. J., Perego, M., Price, S., Quiquet, A., and Ritz, C.: Effect of uncertainty in surface mass balance–elevation feedback on projections of the future sea level contribution of the Greenland ice sheet, *The Cryosphere*, 8, 195–208, doi:10.5194/tc-8-195-2014, 2014a.
- Edwards, T. L., Fettweis, X., Gagliardini, O., Gillet-Chaulet, F., Goelzer, H., Gregory, J. M., Hoffman, M., Huybrechts, P., Payne, A. J., Perego, M., Price, S., Quiquet, A., and Ritz, C.: Probabilistic parameterisation of the surface mass balance–elevation feedback in regional climate model simulations of the Greenland ice sheet, *The Cryosphere*, 8, 181–194, doi:10.5194/tc-8-181-2014, 2014b.
- 25 Fettweis, X., Franco, B., Tedesco, M., van Angelen, J. H., Lenaerts, J. T. M., van den Broeke, M. R., and Gallée, H.: Estimating the Greenland ice sheet surface mass balance contribution to future sea level rise using the regional atmospheric climate model MAR, *The Cryosphere*, 7, 469–489, doi:10.5194/tc-7-469-2013, 2013.
- Fettweis, X., Box, J. E., Agosta, C., Amory, C., Kittel, C., Lang, C., van As, D., Machguth, H., and Gallée, H.: Reconstructions of the 1900–2015 Greenland ice sheet surface mass balance using the regional climate MAR model, *The Cryosphere*, 11, 1015–1033, doi:10.5194/tc-11-1015-2017, 2017.
- 30 Franco, B., Fettweis, X., Lang, C., and Erpicum, M.: Impact of spatial resolution on the modelling of the Greenland ice sheet surface mass balance between 1990–2010, using the regional climate model MAR, *The Cryosphere*, 6, 695–711, doi:10.5194/tc-6-695-2012, 2012.
- Gagliardini, O., Durand, G., Zwinger, T., Hindmarsh, R. C. A., and Le Meur, E.: Coupling of ice-shelf melting and buttressing is a key process in ice-sheets dynamics, *Geophysical Research Letters*, 37, doi:10.1029/2010GL043334, 2010.
- 35



- Gagliardini, O., Zwinger, T., Gillet-Chaulet, F., Durand, G., Favier, L., de Fleurian, B., Greve, R., Malinen, M., Martín, C., Råback, P., Ruokolainen, J., Sacchetti, M., Schäfer, M., Seddik, H., and Thies, J.: Capabilities and performance of Elmer/Ice, a new-generation ice sheet model, *Geoscientific Model Development*, 6, 1299–1318, doi:10.5194/gmd-6-1299-2013, 2013.
- Gallée, H. and Duynkerke, P. G.: Air snow interactions and the surface energy and mass balance over the melting zone of west Greenland during the Greenland Ice Margin Experiment, *Journal of Geophysical Research: Atmospheres*, 102, 13 813–13 824, 1997.
- Gallée, H. and Pettré, P.: Dynamical constraints on katabatic wind cessation in Adélie Land, Antarctica, *Journal of the atmospheric sciences*, 55, 1755–1770, 1998.
- Gallée, H., Pettré, P., and Schayes, G.: Sudden cessation of katabatic winds in Adélie Land, Antarctica, *Journal of Applied Meteorology*, 35, 1142–1152, 1996.
- Gallée, H., Guyomarc'h, G., and Brun, E.: Impact of snow drift on the Antarctic ice sheet surface mass balance: possible sensitivity to snow-surface properties, *Boundary-Layer Meteorology*, 99, 1–19, 2001.
- Gillet-Chaulet, F., Gagliardini, O., Seddik, H., Nodet, M., Durand, G., Ritz, C., Zwinger, T., Greve, R., and Vaughan, D. G.: Greenland ice sheet contribution to sea-level rise from a new-generation ice-sheet model, *The Cryosphere*, 6, 1561–1576, doi:10.5194/tc-6-1561-2012, 2012.
- Howat, I. M., Negrete, A., and Smith, B. E.: The Greenland Ice Mapping Project (GIMP) land classification and surface elevation data sets, *The Cryosphere*, 8, 1509–1518, doi:10.5194/tc-8-1509-2014, 2014.
- Hutter, K.: *Theoretical glaciology: material science of ice and the mechanics of glaciers and ice sheets*, vol. 1, Springer, 1983.
- Huybrechts, P., Janssens, I., Poncin, C., and Fichet, T.: The response of the Greenland ice sheet to climate changes in the 21st century by interactive coupling of an AOGCM with a thermomechanical ice-sheet model, *Annals of Glaciology*, 35, 409–415, 2002.
- Joughin, I., Smith, B. E., Howat, I. M., Scambos, T., and Moon, T.: Greenland flow variability from ice-sheet-wide velocity mapping, *Journal of Glaciology*, 56, 415–430, 2010.
- Kessler, E.: On the distribution and continuity of water substance in atmospheric circulations, in: *On the Distribution and Continuity of Water Substance in Atmospheric Circulations*, pp. 1–84, Springer, 1969.
- Kulesa, B., Hubbard, A. L., Booth, A. D., Bougamont, M., Dow, C. F., Doyle, S. H., Christoffersen, P., Lindbäck, K., Pettersson, R., and Fitzpatrick, A. A.: Seismic evidence for complex sedimentary control of Greenland Ice Sheet flow, *Science Advances*, 3, 2017.
- Lin, Y.-L., Farley, R. D., and Orville, H. D.: Bulk parameterization of the snow field in a cloud model, *Journal of Climate and Applied Meteorology*, 22, 1065–1092, 1983.
- Lunt, D. J., de Noblet-Ducoudré, N., and Charbit, S.: Effects of a melted greenland ice sheet on climate, vegetation, and the cryosphere, *Climate Dynamics*, 23, 679–694, doi:10.1007/s00382-004-0463-4, 2004.
- MacAyeal, D.: Large scale ice flow over a viscous basal sediment: Theory and application to ice stream B, Antarctica, *Journal of Geophysical Research: Solid Earth*, 94, 4071–4087, 1989.
- Machguth, H., Rastner, P., Bolch, T., Mölg, N., Sørensen, L. S., Aðalgeirsdóttir, G., van Angelen, J. H., van den Broeke, M. R., and Fettweis, X.: The future sea-level rise contribution of Greenland's glaciers and ice caps, *Environmental Research Letters*, 8, doi:10.1088/1748-9326/8/2/025005, 2013.
- Maule, C. F., Purucker, M. E., and Olsen, N.: Inferring magnetic crustal thickness and geothermal heat flux from crustal magnetic field models, *Danish Climate Centre Report*, 9, 2009.
- Morcrette, J.-J., Barker, H. W., Cole, J. N. S., Iacono, M. J., and Pincus, R.: Impact of a New Radiation Package, McRad, in the ECMWF Integrated Forecasting System, *Monthly Weather Review*, 136, 4773–4798, doi:10.1175/2008MWR2363.1, 2008.



- Noël, B., van de Berg, W. J., Machguth, H., Lhermitte, S., Howat, I., Fettweis, X., and van den Broeke, M. R.: A daily, 1 km resolution data set of downscaled Greenland ice sheet surface mass balance (1958–2015), *The Cryosphere*, 10, 2361–2377, doi:10.5194/tc-10-2361-2016, 2016.
- Nowicki, S. M. J., Payne, T., Larour, E., Seroussi, H., Goelzer, H., Lipscomb, W., Gregory, J., Abe-Ouchi, A., and Shepherd, A.: Ice Sheet Model Intercomparison Project (ISMIP6) contribution to CMIP6, *Geoscientific Model Development*, pp. 1–42, doi:10.5194/gmd-2016-105, 2016.
- Peano, D., Colleoni, F., Quiquet, A., and Masina, S.: Ice flux evolution in fast flowing areas of the Greenland ice sheet over the 20th and 21st centuries, *Journal of Glaciology*, 63, 499–513, doi:10.1017/jog.2017.12, 2017.
- Peyaud, V., Ritz, C., and Krinner, G.: Modelling the Early Weichselian Eurasian Ice Sheets: role of ice shelves and influence of ice-dammed lakes, *Climate of the Past Discussions*, 3, 221–247, 2007.
- Philippon, G., Ramstein, G., Charbit, S., Kageyama, M., Ritz, C., and Dumas, C.: Evolution of the Antarctic ice sheet throughout the last deglaciation: A study with a new coupled climate—north and south hemisphere ice sheet model, *Earth and Planetary Science Letters*, 248, 750–758, doi:10.1016/j.epsl.2006.06.017, 2006.
- Quiquet, A., Ritz, C., Punge, H. J., and Salas y Méliá, D.: Greenland ice sheet contribution to sea level rise during the last interglacial period: a modelling study driven and constrained by ice core data, *Climate of the Past*, 9, 353–366, doi:10.5194/cp-9-353-2013, 2013.
- Radić, V., Bliss, A., Beedlow, A. C., Hock, R., Miles, E., and Cogley, J. G.: Regional and global projections of twenty-first century glacier mass changes in response to climate scenarios from global climate models, *Climate Dynamics*, 42, 37–58, doi:10.1007/s00382-013-1719-7, 2014.
- Rignot, E., Velicogna, I., Van den Broeke, M., Monaghan, A., and Lenaerts, J.: Acceleration of the contribution of the Greenland and Antarctic ice sheets to sea level rise, *Geophysical Research Letters*, 38, 2011.
- Ritz, C., Rommelaere, V., and Dumas, C.: Modeling the evolution of Antarctic ice sheet over the last 420,000 years: Implications for altitude changes in the Vostok region, *Journal of Geophysical Research: Atmospheres*, 106, 31 943–31 964, 2001.
- Saito, F., Abe-Ouchi, A., Takahashi, K., and Blatter, H.: SeaRISE experiments revisited: potential sources of spread in multi-model projections of the Greenland ice sheet, *The Cryosphere*, 10, 43–63, doi:10.5194/tc-10-43-2016, 2016.
- Serreze, M. C. and Barry, R. G.: Processes and impacts of Arctic amplification: A research synthesis, *Global and Planetary Change*, 77, 85–96, doi:10.1016/j.gloplacha.2011.03.004, 2011.
- Taylor, K. E., Stouffer, R. J., and Meehl, G. A.: An Overview of CMIP5 and the Experiment Design, *Bulletin of the American Meteorological Society*, 93, 485–498, doi:10.1175/BAMS-D-11-00094.1, 2012.
- van den Broeke, M. R. and Gallée, H.: Observation and simulation of barrier winds at the western margin of the Greenland ice sheet, *Quarterly Journal of the Royal Meteorological Society*, 122, 1365–1383, 1996.
- Vizcaino, M., Mikolajewicz, U., Ziemen, F., Rodehacke, C. B., Greve, R., and van den Broeke, M. R.: Coupled simulations of Greenland Ice Sheet and climate change up to A.D. 2300, *Geophysical Research Letters*, 42, 3927–3935, doi:10.1002/2014GL061142, 2015.
- Vizcaíno, M., Mikolajewicz, U., Gröger, M., Maier-Reimer, E., Schurgers, G., and Winguth, A. M. E.: Long-term ice sheet–climate interactions under anthropogenic greenhouse forcing simulated with a complex Earth System Model, *Climate Dynamics*, 31, 665–690, doi:10.1007/s00382-008-0369-7, 2008.
- Watanabe, M., Suzuki, T., O’ishi, R., Komuro, Y., Watanabe, S., Emori, S., Takemura, T., Chikira, M., Ogura, T., Sekiguchi, M., Takata, K., Yamazaki, D., Yokohata, T., Nozawa, T., Hasumi, H., Tatebe, H., and Kimoto, M.: Improved Climate Simulation by MIROC5: Mean States, Variability, and Climate Sensitivity, *Journal of Climate*, 23, 6312–6335, doi:10.1175/2010JCLI3679.1, 2010.

The Cryosphere Discuss., <https://doi.org/10.5194/tc-2017-230>
Manuscript under review for journal The Cryosphere
Discussion started: 6 November 2017
© Author(s) 2017. CC BY 4.0 License.



Weertman, J.: On the sliding of glaciers, *Journal of glaciology*, 3, 33–38, 1957.



Table 1. SMB and ST anomalies between the 2-W coupling experiment and the no coupling experiment (NC) for three periods over their respective ablation zone and ice mask. The value represents the mean anomaly \pm its standard deviation. The area of ice ablation is the area over which SMB is negative for the concerning year.

Anomaly between 2-W and NC anomaly	After 50 yrs	After 100 yrs	After 150 yrs
SMB (cm yr^{-1})	-1.7 ± 6.5	-9.6 ± 16.5	-19.4 ± 31.2
ST ($^{\circ}\text{C}$)	-0.4 ± 0.7	-0.2 ± 0.9	$+0.1 \pm 1.0$
Area of ice ablation (km^2)	-1 800	-6 600	-90 000



Table 2. Ice dynamics anomalies between the 2-W and the NC experiments for three periods. The value represent the mean anomaly \pm its standard deviation.

Anomaly between 2-W and NC anomaly	After 50 yrs	After 100 yrs	After 150 yrs
GrIS Thickness (m)	0 ± 0.9	-2.0 ± 3.4	-9.0 ± 11.1
GrIS ice velocity (m yr^{-1})	-0.5 ± 11.1	-1.1 ± 15.1	-3.0 ± 25.0
GrIS ice sheet area (km^2)	-1 000	-18 300	-52 400

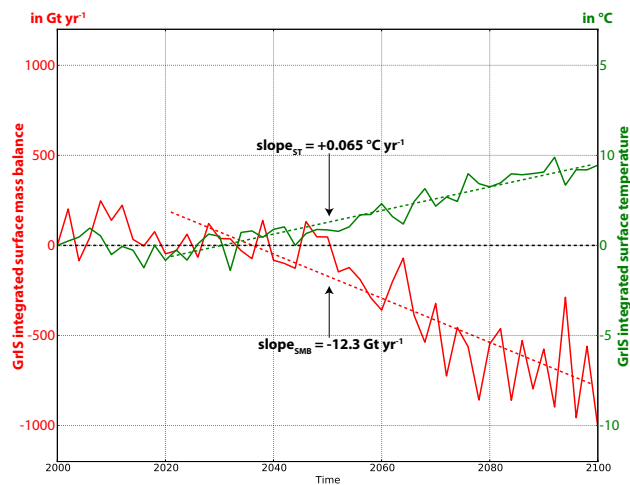


Figure 1. Results for the no coupling experiment. Total surface mass balance in Gt by year over GrIS (red line) and annual surface temperature in Celsius averaged over GrIS (green line) compared to the year 2000. The dashed lines represent the linear interpolation both for ST and SMB over 2020 to 2100.

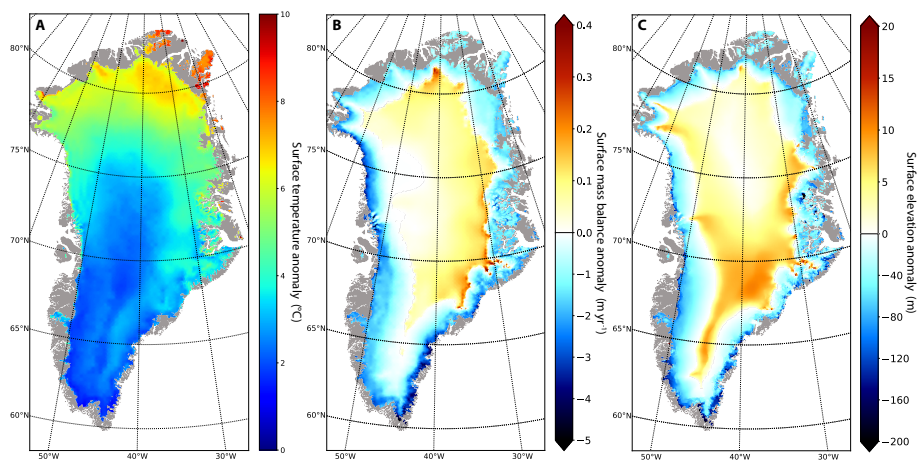


Figure 2. Mean anomalies between the last five years (2095-2100) and the first five years (2000-2005) of the No coupling experiment: (a) Annual surface temperature anomalies °C; (b) Annual surface mass balance anomalies in Gt yr^{-1} ; (c) Surface elevation anomalies in m. The positive scales for the b and c are 10 times lower than the negative scales.

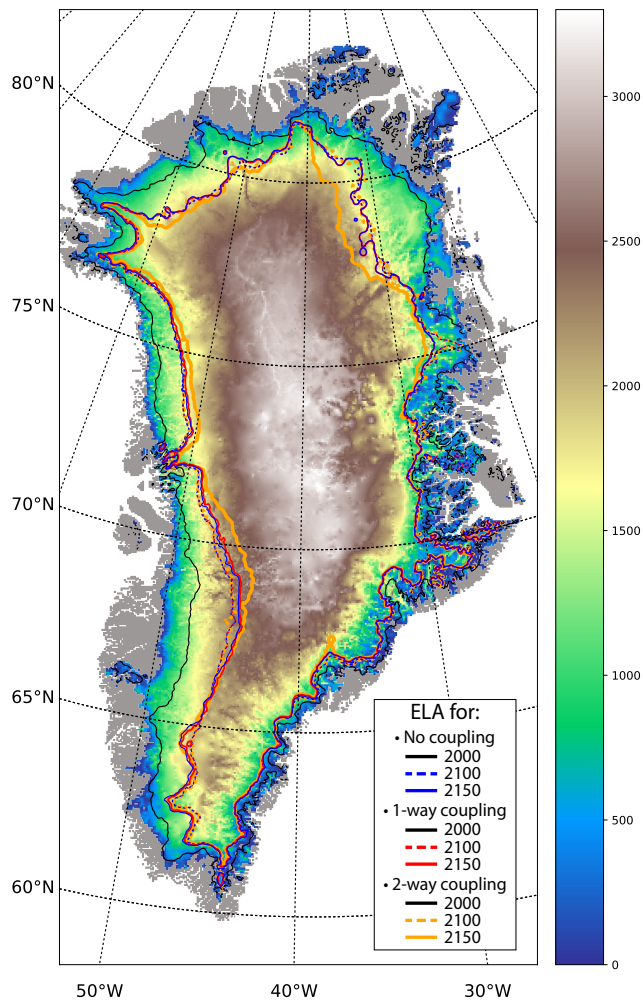


Figure 3. Mean GrIS surface elevation for the last five years (2145-2150) of the 2-W experiment. The solid black line represents the equilibrium line altitude (limit between accumulation and ablation zone) in 2000 for the NC, 1-W and 2-W experiments. The straight and dashed colour lines represent respectively the ELA for the periods 2145-2150 and 2095-2100 for: in blue for the NC experiment ; in red for the 1-W experiment; in orange for the 2-W experiment. The ELA of the 2095-2100 (dashed lines) of NC, 1-W and generally 2-W are superimposed.

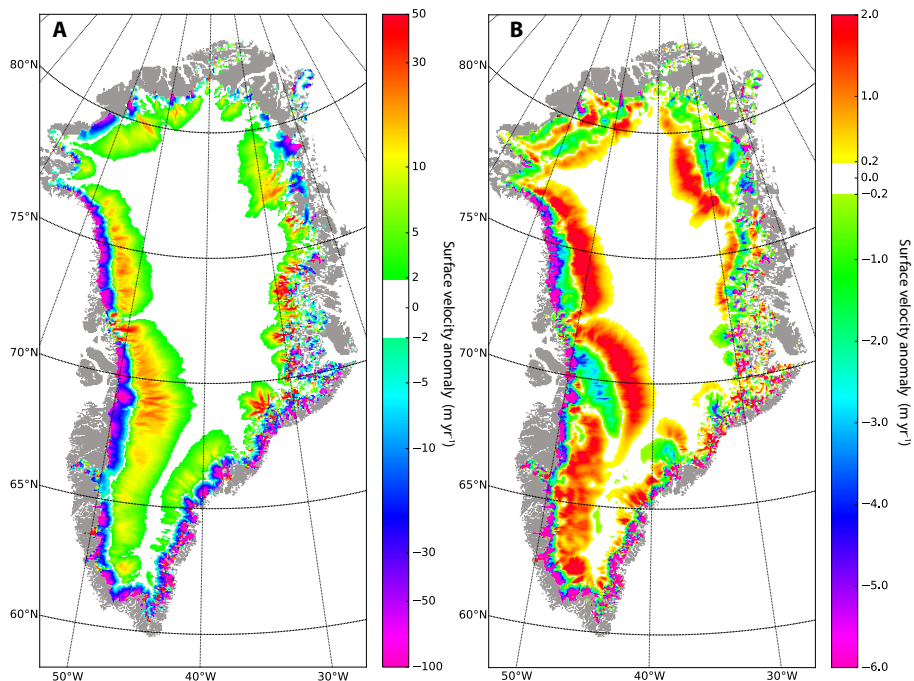


Figure 4. Mean surface velocity anomalies in m yr^{-1} : (a) between the last five years (2095-2100) and the first five years (2000-2005) of the NC experiment; (b) between the last five years (2145-2150) of the 2-W experiment and the last five years (2145-2150) of the NC experiment.

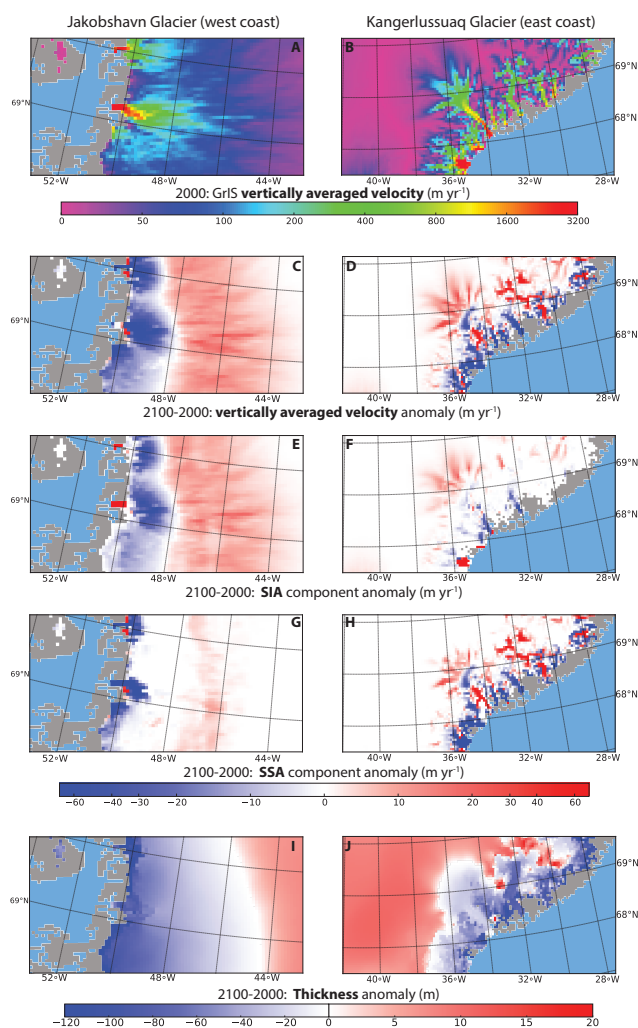


Figure 5. Regional zoom over the Jakobshavn glacier (left panel) and the Kangerlussuaq glacier (right panel) for the NC experiment. (a) and (b) represent the velocity for year 2000. All other figures represent anomaly between the years 2095-2100 and the first five years (2000-2005) of the No coupling experiment: (c) and (d) are the vertically averaged surface velocity anomalies (m yr^{-1}); (e) and (f) are the SIA component anomaly of the averaged velocity (m yr^{-1}); (g) and (h) are the SSA component anomaly of the averaged velocity (m yr^{-1}); (i) and (j) are the GrIS thickness anomaly (m). A logarithmic scale is used for the velocity figures, otherwise we use a linear scale.

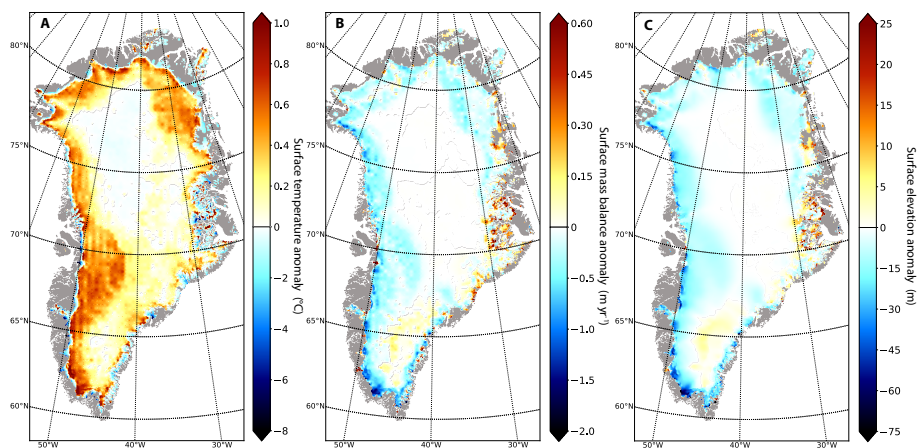


Figure 6. Mean anomalies between the last five years (2145-2150) of the 2-W experiments and the last five years (2145-2150) of the NC experiments: (a) Annual surface temperature anomalies in ° C; (b) Annual surface mass balance anomalies in Gt yr⁻¹; (c) Surface elevation anomalies in m.

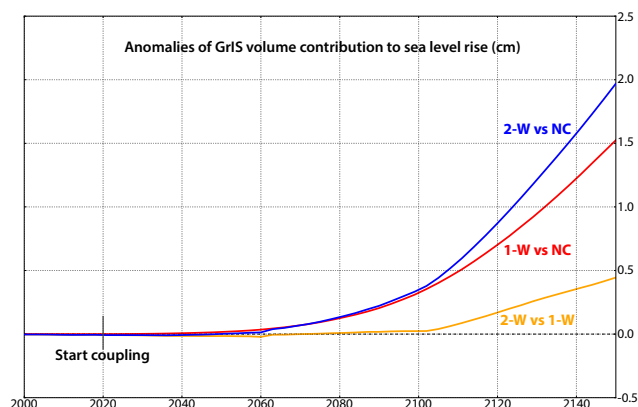


Figure 7. Contribution of the Greenland ice sheet volume contributions to sea level rise (cm) compared to the year 2000 for the three experiments : - Blue line: anomaly between 2-W experiment and no coupling experiment; - red line: anomaly between 1-W experiment and no coupling experiment (NC); - Orange line: anomaly between 2-W coupling experiment and 1-W coupling experiment.

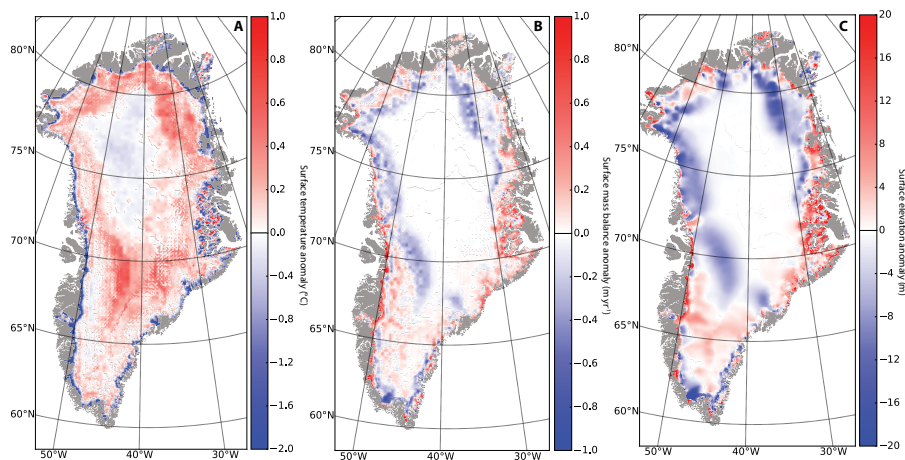


Figure 8. Mean anomalies between the last five years (2145-2150) of the 2-W experiment and the last five years (2145-2150) of the 1-W experiment: (a) Annual surface temperature anomalies in $^{\circ}\text{C}$; (b) Annual surface mass balance anomalies in m yr^{-1} ; (c) Surface elevation anomalies in m.

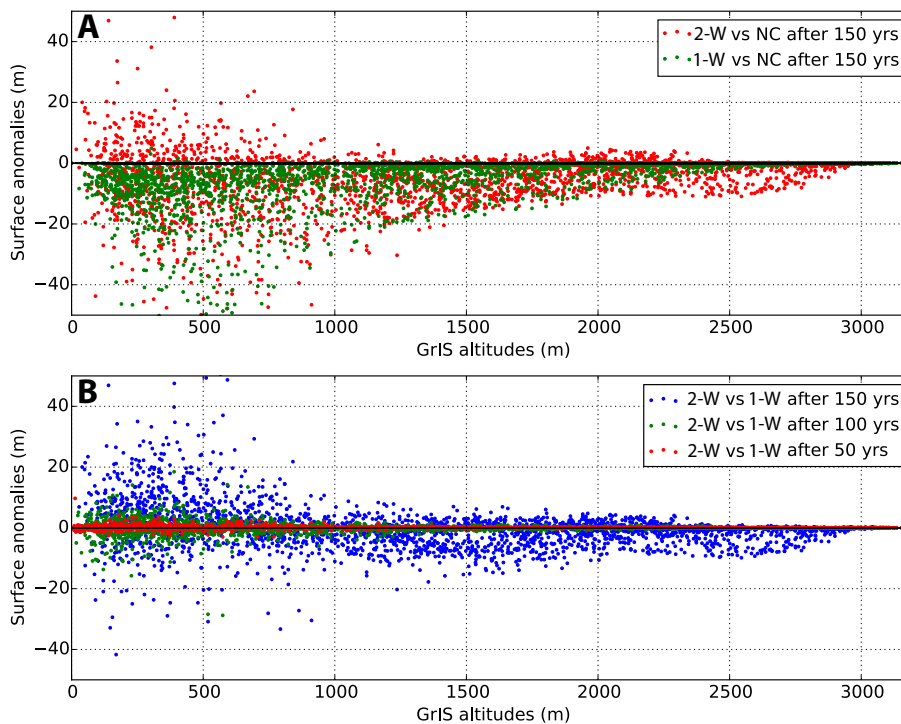


Figure 9. Scatter plot of surface elevation anomalies (m) in function of GrIS surface altitude (m) for the three coupling experiments. In (a) red dots represent surface elevation anomalies between mean 2145-2150 of 2-W experiment and No coupling experiment (NC); green dots is surface elevation anomalies between mean 2145-2150 of 1-W experiment and No coupling experiment (NC). Fig. (b) represents surface elevation anomalies between 2-W experiment and 1-W experiment for respectively : in red dots mean 2045-2050; in green dots mean 2095-2100; blue dots mean 2145-2150.